

Static fatigue of rubbery polymers: statistical approach to the failure process

K. FUKUMORI, T. KURAUCHI

Toyota Central Research and Development Laboratories, Inc, Nagakute-cho, Aichi-gun, Aichi-ken, 480-11, Japan

A phenomenological theory of a stochastic process was applied to the study of the failure mechanism of static fatigue of rubbery polymers. Static fatigue, namely, creep and stress relaxation experiments, were made on two specimens, pure vulcanizate and carbon-reinforced vulcanizate of acrylonitrile-butadiene rubber (NBR). The distributions of the lifetime were analysed by means of the function in the form of the Weibull distribution, which is an improvement of the stochastic theory proposed by Kawabata *et al.* The experiments proved the validity of the theory. Furthermore, the experimental results suggest that, in pure vulcanizate, a critical crack initiates and propagates unstably (random process at Weibull modulus of unity), and that, in carbon-reinforced vulcanizate, multi-cracks initiate and propagate stably due to the presence of carbon black particles (wear-out process at Weibull modulus of 1 to ~ 3). The scattering in the lifetime of pure vulcanizate seems to reflect the inherent characteristics of the polymer.

1. Introduction

It is well-known that the strength of solid materials scatters remarkably even under identical conditions. Hence, for prediction of the lifetime of those materials, knowledge of the distribution function as well as its dependence on stress state is required. The purpose of this study is to estimate the failure mechanism of pure vulcanizate and the reinforcement mechanism of carbon black particles in the vulcanizate by application of the statistical analysis.

In polymeric solids, the viscoelastic effect is observed in the failure behaviour as well as in the mechanical properties. Therefore, the failure behaviour depends on time mainly through the following two factors. One is that the viscoelasticity in the mechanical properties has indirect influence on the failure behaviour, and the other is that the failure mechanism itself, e.g. crack propagation, depends on time. Actually, however, both factors may be combined, which makes the study of the mechanism difficult. The factors should be separately studied to clarify the failure. Figs. 1a and b are schematic representations of creep and stress relaxation behaviours of rubber

vulcanizates. As shown in the figures, the strain, ϵ , or the stress, σ , seems to be kept nearly constant (ϵ_0 or σ_0), and plastic deformation seems to be absent at the final stage of the failure in both processes. Therefore, in static fatigue, failure occurs suddenly under the stress state of the nearly constant true stress. Thus, it is considered that the independent observation of the time dependence of the failure mechanism alone can be made in static fatigue.

In this work, static fatigue of rubber vulcanizates was studied and analysed on the basis of the stochastic theory. The determination of the distribution function of the lifetime and observation of the fracture surface were made. The failure mechanism of static fatigue was estimated from the results.

2. Theoretical considerations

Stochastic theory has been applied to various types of failure, e.g. creep failure in concretes by Hori [1, 2], tensile failure, creep failure, etc., in polymeric fibres by Coleman [3-5] and Narisawa *et al.* [6], and failure in semicrystalline polymers by Kausch [7]. For rubbery polymers, Kawabata

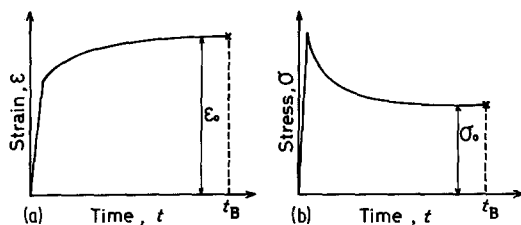


Figure 1 Schematic representation of static fatigue of rubber vulcanizates. ϵ_0 , constant strain; σ_0 , constant stress; t_B , time-to-break (lifetime).

et al. [8–10] developed a stochastic theory of creep failure. In spite of the simplicity of the theory, it is very fruitful for the study of the polymers. This theory, however, seems to have to be modified for the study of the static fatigue of rubbery polymers, especially for that of the reinforcement mechanism by carbon black particles.

Generally, it is supposed that there are many pre-existing flaws distributed randomly in rubber vulcanizates. In the theory by Kawabata *et al.*, the flaws are assumed to appear and disappear with time in the viscoelastic body under a constant stress state, i.e. in creep and stress relaxation processes. In addition to this assumption, Kawabata *et al.* assume that if any one cell containing only a few flaws in a unit volume falls into a critical state and makes a crack, the crack propagates instantaneously through the whole body, causing a catastrophic failure of the solid immediately. The theory is based on the weakest link concept that the failure of a solid is determined by the strength of its weakest volume element. On these assumptions, the probability density function of the lifetime, $f(t)$, is given by the following, on the basis of a stochastic theory [11, 12]:

$$f(t) = \mu_0 \exp(-\mu_0 t) \quad (1)$$

where t is time and μ_0 is a constant. The validity of Equation 1 has been proved experimentally for pure vulcanizate [8–10].

For carbon-reinforced vulcanizate, the second assumption is modified as follows, considering the interaction between rubber and filler: assuming independence of initiations of ν cracks, the occurrence of multi-cracks (ν) in a unit volume causes the failure of the solid. The probability density function of the lifetime, $f(t)$, can be expressed as

$$f(t) = \frac{1}{\Gamma(\nu)} \mu_0^\nu t^{\nu-1} \exp(-\mu_0 t) \quad (2)$$

where Γ is the gamma function. The validity of Equation 2 is proved experimentally, in which ν is selected as 3 or 4 to fit the experimental results [9, 10].

As mentioned above, the theory for the failure mechanism of rubber vulcanizates implies that a critical crack may initiate and propagate only at a portion of a specimen. For carbon-reinforced vulcanizate, however, it is often observed that there are many portions where visible macrocracks initiate prior to failure under a constant strain rate test condition; yet it is rarely observed for pure vulcanizate. This suggests that multi-cracks possibly may initiate in addition to the crack interruption [9, 10, 13–15] in carbon-reinforced vulcanizate. Therefore, modification of the theory of Kawabata *et al.* might be necessary on this aspect. It is assumed that multiple (n) sites, from which the failure of the solid can originate, exist in the solid, that in any one of the sites ν mutually independent microcracks occur, that the smallest value of $t_{\nu, q}$ determines the lifetime of the solid, where $t_{\nu, q}$ stands for the time in which the number of the microcracks reaches ν in the q th-site ($q = 1, 2, \dots, n$), and that the period of the crack growth in the final stage of the failure is small in comparison with $t_{\nu, q}$.

On this assumption, the statistical distribution of the lifetime would be obtained as the distribution of the smallest value of the initial distribution $f_0(t)$ (the gamma distribution) in sites of size n ($n \geq 1$). In this case, finally, the distribution for the smallest value of $t_{\nu, q}$, i.e. the probability of survival, $R(t)$, is obtained as the limited form [16]:

$$R(t) \cong \exp \left[-n \int_0^t f_0(t) dt \right] \cong \exp \left[-\left(\frac{t}{\beta} \right)^m \right] \quad (3)$$

where β and m are constants. The functional form of Equation 3 corresponds to that of Weibull distribution, or the distribution of the third asymptotic type. Hence, from Equation 3, the transition probability, or the failure rate, $\mu(t)$, is given by

$$\mu(t) = \frac{-dR(t)/dt}{R(t)} = \frac{mt^{m-1}}{\beta^m} \quad (4)$$

For $m = 1$, Equation 4 can be written as

$$\mu(t) = \frac{1}{\beta} (= \text{constant}) \quad (5)$$

Hence, the probability density function, $f(t)$, is

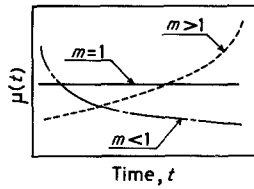


Figure 2 Failure rate, $\mu(t)$, plotted against time for three ranges of m (schematic), m , Weibull modulus.

obtained as

$$f(t) = \mu(t) \exp \left[- \int_0^t \mu(t) dt \right] = \frac{1}{\beta} \exp \left(- \frac{t}{\beta} \right) \quad (6)$$

The functional form of Equation 6 is identical with that of Equation 1. Therefore, the functional form of Equation 3, or Weibull distribution, may express the stochastic process of the failure for pure vulcanizate as well as that for carbon-reinforced vulcanizate.

In Weibull's expression, the failure rate, $\mu(t)$, indicates three types of failure mode [17] corresponding to three ranges of m as shown in Fig. 2:

$m = 1$. . . random failure (constant failure rate)

$m > 1$. . . wear-out failure (increasing failure rate)

$m < 1$. . . initial failure (decreasing failure rate)

Thus, by evaluation of the shape parameter, or Weibull modulus, m , in Equation 3, the influence of stress state and the carbon-reinforcement on the failure mechanism can be estimated. Moreover, this theory could be useful in discussing the spatial distribution of flaws in the solid as well as the time dependence of the initiation of the microcracks leading to failure, in a similar way to the study of failure in metals by Yokobori and Sawaki [18, 19].

3. Experimental procedure

3.1. Materials

The materials used to test the theory are pure acrylonitrile-butadiene rubber (NBR) vulcanizate and carbon-reinforced NBR vulcanizate. The composition of specimens and the vulcanization conditions are shown in Table I. Ring specimens were punched out from the compression-moulded sheets 1 or 2 mm thick. The dimensions of these are shown in Table II.

3.2. Measurement of time-to-break (lifetime), t_B

Static fatigue experiments were carried out at

TABLE I Composition of specimens and condition of vulcanization

Symbol	SP-NBR	SC-NBR
NBR (AN = 33%)	100 phr	100 phr
ZnO	5	5
St. acid	1	1
Carbon (SRF)	—	40
S	1.5	1.5
Accelerator	1	1

Notes

phr: parts per hundred parts of rubber by weight.

AN: Acrylonitrile.

Cure condition: 15 min at 160°C.

23°C in ambient atmosphere. Fig. 3 shows schematic diagrams of the measurement of the lifetime, t_B . As shown in Fig. 3a, in a creep experiment, a constant load or constant engineering stress, σ_e , was applied to a specimen with the use of a dead load. In a stress relaxation experiment, a specimen was held at a constant stretch ratio, λ , as shown in Fig. 3b. The test conditions are shown in Table III. The measurement of the lifetime, t_B , was made on 20 specimens under each test condition.

3.3. Observation of fracture surfaces

Fracture surfaces of specimens were observed with scanning electron microscope (SEM). To get a clear image, fracture surfaces were sputter-coated with gold.

4. Results

4.1. Weibull plot of the distribution of the lifetime, t_B

The fitness of Weibull distribution to express the distribution of the lifetime for rubber vulcanizates is first examined. Equation 3 can be transformed into

$$\ln [-\ln R(t)] = m \ln t - m \ln \beta \quad (7)$$

Following Gumbel [16], the cumulative distribution of the lifetime, $F(t_i)$, where t_i is the i th failure time, is obtained as follows:

$$F(t_i) = \frac{i}{N+1} \quad (8)$$

TABLE II Dimensions of specimens

	Diameter (mm)		Volume (mm ³)
	Outside	Inside	
SP-NBR	22.0	19.0	169.3
SC-NBR	20.0	18.6	35.0

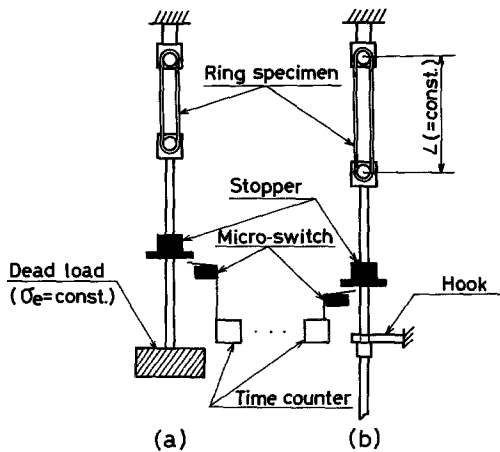


Figure 3 Schematic diagrams of the apparatus for measurement of lifetime: (a) creep; (b) stress relaxation.

where N is the number of specimens tested. Hence, the probability of survival, $R(t_i)$, is given by

$$R(t_i) = 1 - F(t_i) = \frac{N + 1 - i}{N + 1} \quad (9)$$

Substituting Equation 9 into Equation 7, the following equation is obtained:

$$\ln \left[\ln \left(\frac{N + 1}{N + 1 - i} \right) \right] = m \ln t_i - m \ln \beta \quad (10)$$

Following Equation 10, $\ln[-\ln R(t_i)] (= \ln \{ \ln [(20 + 1)/(20 + 1 - i)] \})$ is plotted against $\ln t_i$ in stress relaxation experiments for SP-NBR and SC-NBR, i.e. Weibull plot, as shown in Fig. 4. As seen in this figure, the observed values for SP-NBR and SC-NBR appear to give a good fit to a straight line, which proves that the Weibull distribution is appropriate to express the experimental results.

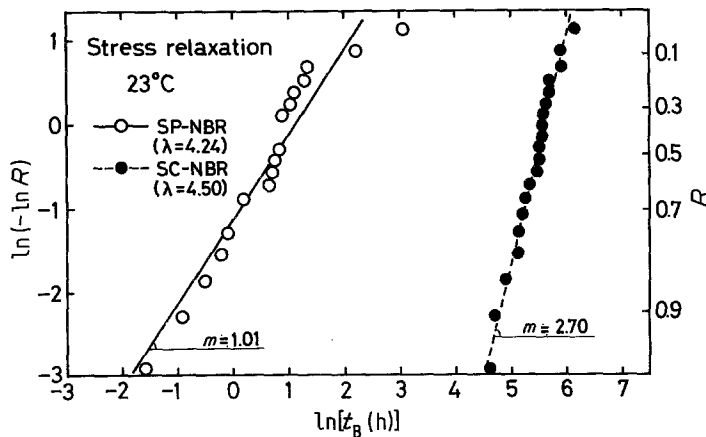


Figure 4 Typical Weibull plots of the distribution of the lifetime, t_B , in stress relaxation for SP-NBR and SC-NBR [plot of $\ln(-\ln R)$ against $\ln t_B$]. R , probability of survival; λ , constant stretch ratio. The values of Weibull modulus, m , were evaluated by taking least-squares.

TABLE III Test conditions

	SP-NBR	SC-NBR
Creep,	0.686, 0.934	5.88, 11.76
σ_e (MPa)	0.750, 1.323	7.84, 14.70
	0.784, 1.695	9.80, -
Stress relaxation,	3.00, 5.17	4.50, 6.00
λ	3.62, 5.79	5.00, 6.50
	4.24, -	5.50, 7.00

σ_e , constant engineering stress.
 λ , constant stretch ratio.

Thus, the Weibull plots of the distribution of the lifetime for SP-NBR and SC-NBR under all test conditions were examined as shown in Fig. 4. The results for SP-NBR and SC-NBR are shown in Figs. 5 to 8. From the slope of the Weibull plot, the Weibull modulus, m , was determined by taking least-squares according to Equation 7.

4.2. Relationship between m and the mean lifetime, $\langle t_B \rangle$

The mean lifetime, $\langle t_B \rangle$, is calculated from β and m , using Equation 4, as follows:

$$\begin{aligned} \langle t_B \rangle &= \int_0^{\infty} t \cdot f(t) dt \\ &= \int_0^{\infty} t [\mu(t)] \int_0^t \mu(t) dt dt \\ &= \beta \cdot \Gamma(1 + 1/m) \end{aligned} \quad (11)$$

where Γ is the gamma function. The value of m is plotted against the mean lifetime, $\langle t_B \rangle$, in Fig. 9, for SP-NBR and SC-NBR under each test condition. From this figure, the dependence of m on $\langle t_B \rangle$ for SP-NBR and SC-NBR is clearly seen. It shows that m also depends on the stress state.

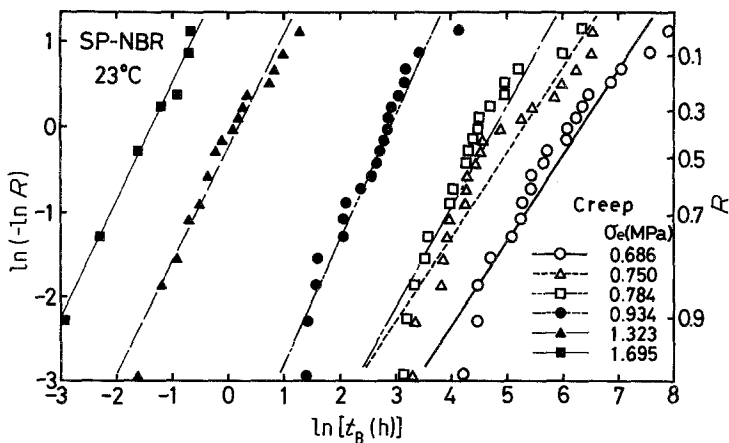


Figure 5 Weibull plots of the distribution of the lifetime, t_B , for SP-NBR tested under creep conditions (constant engineering stress, σ_e). R , probability of survival.

For SP-NBR, the value of m appears to range from about 0.95 to 1.35. In the stress relaxation experiments, the value of m nearly equals 1.0 over a wide range of $\langle t_B \rangle$. In the creep experiments, it equals about 1.35 in a short-term failure, but approaches 1.0 in a long-term failure. Thus, it can be concluded that the value of m equals 1.0 for SP-NBR, although it is thought that there might be some difference between the failure behaviour in the creep process and that in the stress relaxation process, in the short-term failure. According to Equation 4, it is known that the failure rate, $\mu(t)$, is constant against time, which means that the failure probability is kept constant in any unit time. Hence, it is considered that the failure behaviour in pure vulcanizate may be of the random process ($m = 1$).

For SC-NBR, as seen in Fig. 9, the value of m depends strongly on $\langle t_B \rangle$. In the short-term failure, the failure behaviour may be of a random process in a similar manner to that in pure vulcanizate, while, in the long-term failure, it gradually

approaches ~ 3.0 , which implies that the failure behaviour changes to the wear-out process ($m > 1$). In the latter case, the failure rate, $\mu(t)$, increases monotonically with time. Moreover, the difference between the failure behaviour in the creep process and that in the stress relaxation process seems to be more remarkable than that in pure vulcanizate. For $\langle t_B \rangle > 10^2$ h, however, it is considered that both processes may have almost the same characteristics in the failure behaviour.

4.3. Fracture surfaces

Scanning electron micrographs of fracture surfaces of SP-NBR are given in Fig. 10a for the creep experiment and in Fig. 10b for the stress relaxation experiment. These figures show the characteristic features of brittle fracture. Brittle fracture traverses through the matrix and leaves some cleavage patterns, where there are some inhomogeneities in the material. But, in the smooth fracture surfaces, any evident traces of the crack initiation can hardly be recognized. It is con-

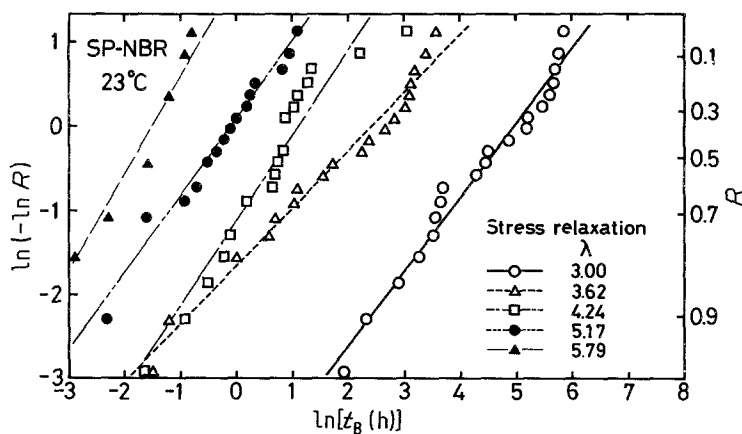


Figure 6 Weibull plots of the distribution of the lifetime, t_B , for SP-NBR tested under stress relaxation conditions (constant stretch ratio, λ). R , probability of survival.

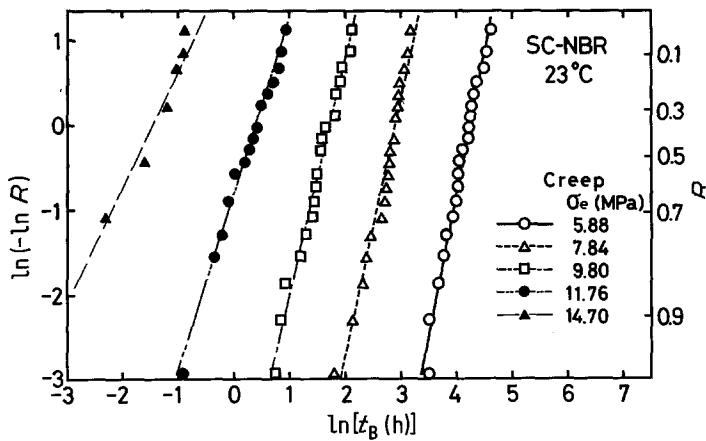


Figure 7 Weibull plots of the distribution of the lifetime, t_B , for SC-NBR tested under creep conditions (constant engineering stress, σ_e). R , probability of survival.

considered that a crack in the abrupt failure propagates unstably along a wide front. These features of fracture surfaces of SP-NBR are almost the same under all test conditions (creep, stress relaxation) with those shown in Figs. 10a and b. Thus, it is suggested that, in pure vulcanizate, a critical crack may propagate unstably and that the failure behaviour may be of the random process, corresponding to the value of $m (\approx 1)$.

Scanning electron micrographs of fracture surfaces of SC-NBR are shown in Figs. 11 and 12. First, Figs. 11a and b show fracture surfaces from creep and stress relaxation experiments in the long-term failure, respectively. These features of fracture surfaces evidently differ from those of SP-NBR. Owing to the presence of carbon black particles which causes mechanical hysteresis, normal stresses distributed unevenly over a cross-sectional area may cause the material to tear from the surface or macrocrack originating from microcracks or flaws in the matrix. As evidence of the tear fracture, chevron patterns are observed

on the fracture surface, and their tips point in the direction opposite to the crack propagation. These features of fracture surfaces in carbon-reinforced vulcanizate appear to be the same in both creep and stress relaxation experiments. Chevron patterns are made when the crack propagation is interrupted locally and the patterns are absent in pure vulcanizate. Therefore, carbon black particles may be thought to be able to sustain stable cracks or interrupt the unstable (or catastrophic) crack propagation, which corresponds to the wear-out failure ($m > 1$).

Secondly, as shown in Figs. 12a (creep) and b (stress relaxation), in the short-term failure, the features of fracture surfaces are quite different from those in the long-term failure: there is little evidence of tear fracture, and a macro-critical crack initiates and propagates widely, which seems to indicate that there is no slow crack propagation. Hence, it is supposed that, in the short-term failure, or at high stress levels, carbon black particles may be incapable of interrupting the

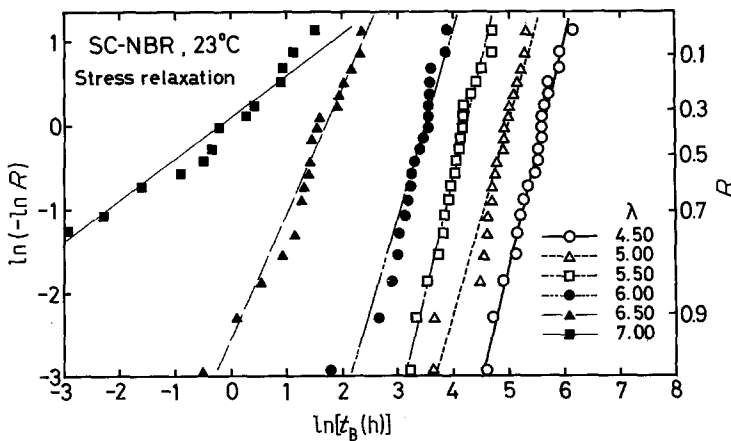


Figure 8 Weibull plots of the distribution of the lifetime, t_B , for SC-NBR tested under stress relaxation conditions (constant stretch ratio, λ). R , probability of survival.

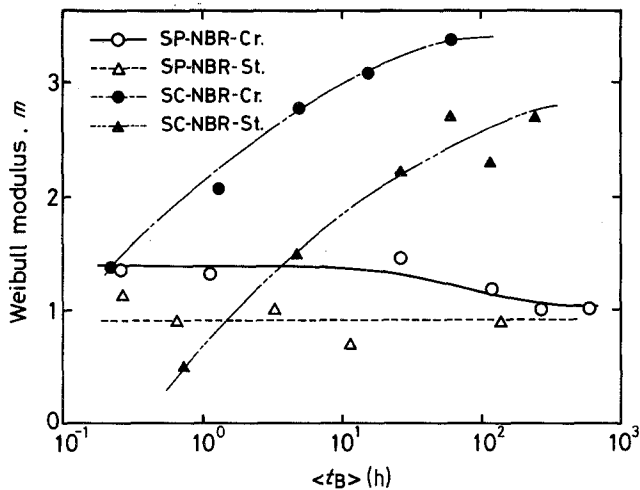


Figure 9 Plots of m against $\langle t_B \rangle$ for SP-NBR and SC-NBR. $\langle t_B \rangle$, mean lifetime; Cr, creep; St, stress relaxation.

unstable crack propagation, in contrast with the long-term failure. In short-term failure, it is considered that the failure behaviour may be of the random process ($m = 1$).

From the results mentioned above, it may be concluded that there is a good correlation between the values of m and the features of fracture surfaces. It is suggested that a change in the failure statistics may reflect the change in the failure mode or type.

4.4. Appearances of broken specimens

Typical appearances of broken specimens are shown schematically in Fig. 13. Fig. 13a shows that a specimen breaks transversely against the direction of the applied stress without any plastic deformation in pure vulcanizate. In contrast, it is seen in Fig. 13b for carbon-reinforced vulcanizate

that there is some deviation from a direct tear path, termed “knotty” tearing [13, 14]. This form of tearing seems to be caused by the discontinuous stick–slip process. It is suggested that the material may locally attain some oriented structure due to an increase in the heterogeneity of the tear. Furthermore, in contrast to pure vulcanizate, it was observed that there were many cracks initiated on the surface of the specimen. It infers the possibility of multi-crack initiation in carbon-reinforced vulcanizate. Thus, it is considered that the reinforcement by carbon black particles may result from the influence of hysteresis on the stress concentration near the tip of tearing or growing cracks, and that, in addition, the dispersed particles may serve to interrupt or blunt the crack propagation through the spatial effects, delaying the onset of the catastrophic failure.

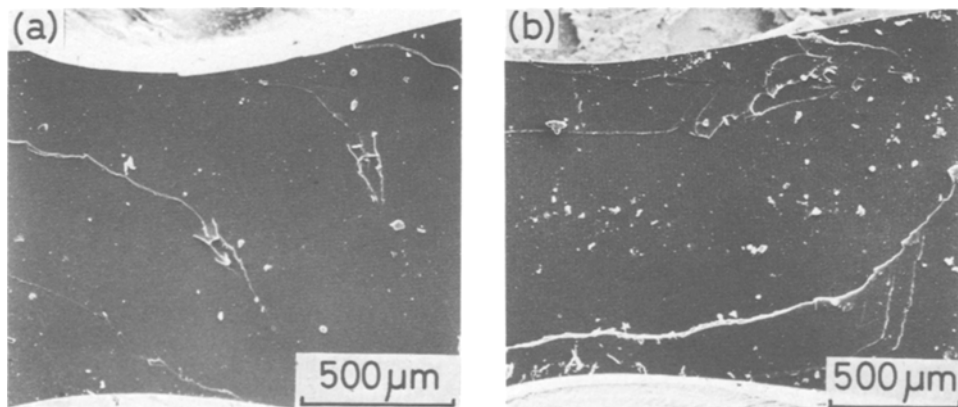


Figure 10 Scanning electron micrographs of fracture surfaces of SP-NBR in: (a) creep ($\sigma_e = 0.686$ MPa, $t_B = 306.9$ h), (b) stress relaxation ($\lambda = 4.24$, $t_B = 21.4$ h). t_B , lifetime; σ_e , constant engineering stress; λ , constant stretch ratio.

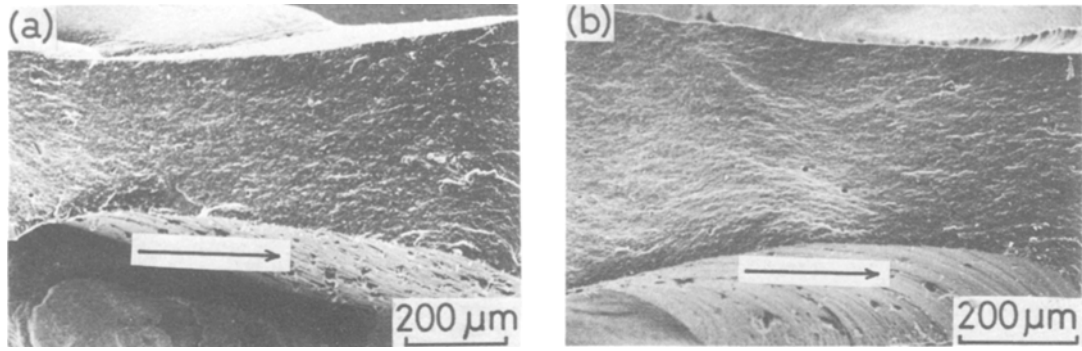


Figure 11 Scanning electron micrographs of fracture surfaces of SC-NBR (long-term failure) in: (a) creep ($\sigma_e = 5.88$ MPa, $t_B = 56.4$ h); (b) stress relaxation ($\lambda = 4.50$, $t_B = 247.9$ h). t_B , lifetime; σ_e , constant engineering stress; λ , constant stretch ratio. Arrows indicate the direction of crack propagation (tearing).

5. Discussion

5.1. Dependence of the mean lifetime $\langle t_B \rangle$ on the applied true stress, σ_t

Theoretically or experimentally [1–6, 8–10, 18, 19], the relationship between the failure rate, $\mu(t)$, in Equation 4 and the applied true stress, $\sigma_t(t)$, is given by

$$\mu(t) = VC(t)[\sigma_t(t)]^n \quad (12)$$

where n is a material constant, V is the stressed volume of the specimen, and $C(t)$ is a function representing the dependence of the crack length, temperature, environmental effects, etc., on time, but independent of stress. For rubber vulcanizates, it is assumed that the true stress, $\sigma_t(t)$, is nearly constant against time in some period prior to the break in creep and stress relaxation processes.

Hence, Equation 12 is transformed into

$$\mu(t) = VC(t)\sigma_{t0}^n \quad (13)$$

where σ_{t0} is a constant. From Equations 4, 11 and 13, the interrelation between the mean lifetime, $\langle t_B \rangle$, and the constant true stress, σ_{t0} , is obtained as follows:

$$\langle t_B \rangle = A/\sigma_{t0}^{n/m} \quad (14)$$

or

$$\log \sigma_{t0} = -\frac{m}{n} \log \langle t_B \rangle + \frac{m}{n} \log A \quad (15)$$

where A is a constant. The value of σ_{t0} is not always the same for each specimen, and for the prediction of the mean lifetime, the mean breaking true stress, $\langle \sigma_{tb} \rangle$, is to be substituted for σ_{t0} .

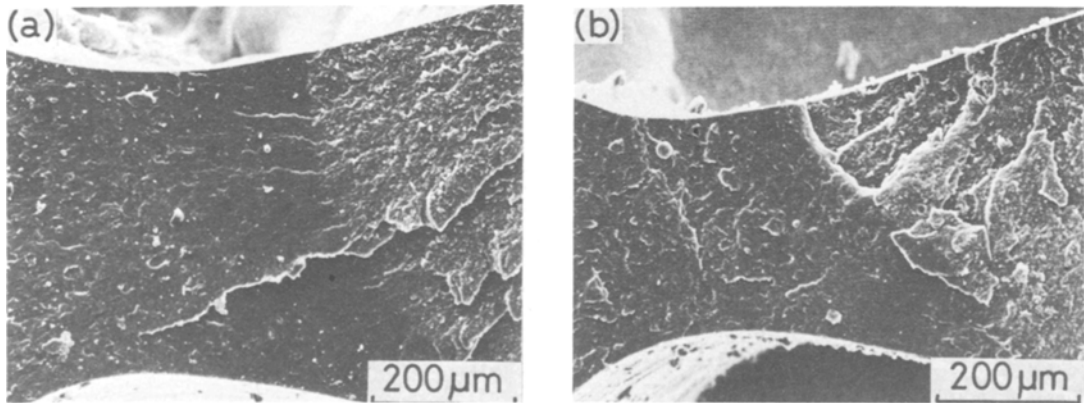


Figure 12 Scanning electron micrographs of fracture surfaces of SC-NBR (short-term failure) in: (a) creep ($\sigma_e = 14.7$ MPa, $t_B = 0.3$ h); (b) stress relaxation ($\lambda = 7.00$, $t_B = 0.7$ h). t_B , lifetime; σ_e , constant engineering stress; λ , constant stretch ratio.

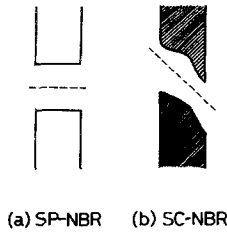


Figure 13 Typical appearances of broken specimens (schematic).

Hence,

$$\log\langle\sigma_{tb}\rangle = -\frac{m}{n}\log\langle t_B\rangle + \frac{m}{n}\log A \quad (15a)$$

Here, the mean breaking true stress, $\langle\sigma_{tb}\rangle$, is approximately calculated by the following equations [10]:

$$\langle\sigma_{tb}\rangle \approx \begin{cases} \sigma_e\langle\lambda_b\rangle & \text{in creep} \\ \langle\sigma_{eb}\rangle\lambda & \text{in stress relaxation} \end{cases} \quad (16)$$

where $\langle\lambda_b\rangle$ is the mean breaking stretch ratio and $\langle\sigma_{eb}\rangle$ is the mean breaking engineering stress. Using Equations 15a to 17, $\log\langle\sigma_{tb}\rangle$ plotted against $\log\langle t_B\rangle$ for SP-NBR and SC-NBR are shown in Figs. 14 and 15, respectively.

As seen in Fig. 14, for SP-NBR, $\log\langle\sigma_{tb}\rangle$ plotted against $\log\langle t_B\rangle$ gives a straight line in accordance with Equation 15a. Thus, it is concluded that the dependence of $\langle t_B\rangle$ on $\langle\sigma_{tb}\rangle$ may be nearly the same in both creep and stress relaxation processes for pure vulcanizate. In the figure, the material constant, n , can be evaluated from the slope of the straight line: the evaluated value of n is about 3.99.

On the other hand, $\log\langle\sigma_{tb}\rangle$ plotted against

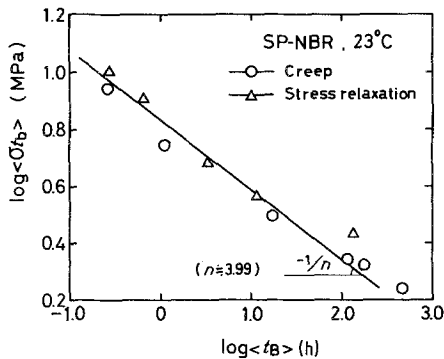


Figure 14 Plot of $\log\langle\sigma_{tb}\rangle$ against $\log\langle t_B\rangle$ for SP-NBR. $\langle\sigma_{tb}\rangle$, mean breaking true stress; $\langle t_B\rangle$, mean lifetime; n , material constant. The value of n was evaluated from the slope of the plot.

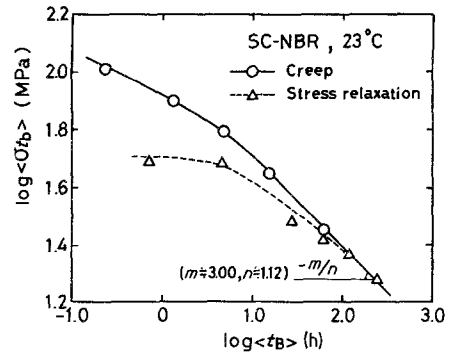


Figure 15 Plot of $\log\langle\sigma_{tb}\rangle$ against $\log\langle t_B\rangle$ for SC-NBR. $\langle\sigma_{tb}\rangle$, mean breaking true stress; $\langle t_B\rangle$, mean lifetime; n , material constant; m , Weibull modulus. The value of n was evaluated from the slope of the linear portion of the plot where m was put at 3.0.

$\log\langle t_B\rangle$ for SC-NBR does not give a straight line, as shown in Fig. 15. Especially in the range of the short-term failure in the stress relaxation process, or at high stress levels, much deviation from the linear relation occurs. It is supposed that the occurrence of the deviation in SC-NBR may be caused by the following two factors:

1. the failure behaviour of carbon-reinforced vulcanizate depends on the stress state as already mentioned, i.e. it changes to be of the random process ($m = 1$) in the short-term failure from the wear-out process ($m > 1$) in the long-term failure;
2. the applied true stress in the stress relaxation process has a maximum value at the time when the strain is complete (constant stretch ratio, λ), while in the creep process, it is at a maximum at break. As seen in Fig. 15, the failure behaviour in the stress relaxation process differs remarkably at high stress levels from that in the creep one. This suggests that the stress relaxation process, especially at high stress levels, may be connected with the irreversible change of the structure after the first application of strain, in contrast to the creep process. It is considered that it may be caused by the progressive detachment of weak bondings, i.e. breaking of network chains in interaction with carbon black particles, etc. [20].

In long-term failure important in engineering practice, however, $\log\langle\sigma_{tb}\rangle$ plotted against $\log\langle t_B\rangle$ yields virtually a straight line. In this portion, it seems that the dependence of $\langle t_B\rangle$ on $\langle\sigma_{tb}\rangle$ may be similar in both creep and stress relaxation processes as well as that for pure vulcanizate. The value of n is evaluated as 1.12 from the slope of this portion of the plot, where the value of m is put at 3.0.

The material constant, n , obtained is concerned with the relationship between the failure rate, $\mu(t)$, and the true stress σ_t , as shown in Equation 13. As shown above, the value of n obtained for carbon-reinforced vulcanizate ($n \doteq 1.12$) is lower than that obtained for pure vulcanizate ($n \doteq 3.99$), in long-term failure. Therefore, in engineering practice, it is estimated that the failure behaviour of carbon-reinforced vulcanizate may be relatively insensitive to the change in true stress in comparison with that of pure vulcanizate.

5.2. Effect of viscoelasticity on the distribution of the lifetime, t_B

Although it has been assumed that the true stress, σ_t , is constant against time in both creep and stress relaxation processes, it will change slightly monotonically with time: it increases in the creep process and decreases in the stress relaxation process with time. Thus, to examine the effect of viscoelasticity in the distribution of the lifetime, t_B , the mechanical behaviour of the rubber vulcanizates used here was observed.

The mechanical behaviour of rubber vulcanizates in creep and stress relaxation processes is empirically approximated by the following equations, respectively [10]:

$$\lambda(t) = \lambda_0 t^{k_c} \quad \text{in creep, for the case of large } \lambda \quad (18)$$

$$\sigma_e(t) = \sigma_0 t^{-k_r} \quad \text{in stress relaxation} \quad (19)$$

where λ_0 , σ_0 , k_c and k_r are constants. Hence, from Equations 18 and 19, the true stress, $\sigma_t(t)$, in both processes are obtained as

$$\sigma_t(t) \simeq \begin{cases} \sigma_e \lambda(t) = \sigma_e \lambda_0 t^{k_c} & \text{in creep} \\ \sigma_e(t) \lambda = \sigma_0 \lambda t^{-k_r} & \text{in stress relaxation} \end{cases} \quad (20)$$

$$(21)$$

respectively. In these cases, comparing the failure rate, $\mu(t)$, in Equation 4 with Equations 12, 20 and 21, the Weibull modulus, m , can be divided into two terms as follows:

$$m = m' + nk \quad (22)$$

where m' is a constant, and k equals k_c (the creep rate) in the creep process and $-k_r$ (the stress relaxation rate) in the stress relaxation process, respectively. That is, k corresponds to the effect of viscoelasticity.

The dependence of the creep rate, k_c , or the stress relaxation rate, k_r , on the mean lifetime

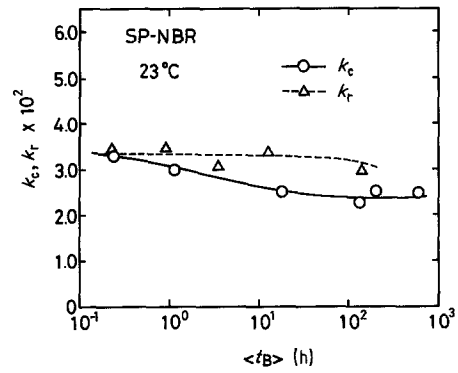


Figure 16 k_c and k_r plotted against $\langle t_B \rangle$ for SP-NBR. k_c , creep rate; k_r , stress relaxation rate; $\langle t_B \rangle$, mean lifetime.

$\langle t_B \rangle$, for SP-NBR and SC-NBR is shown in Figs. 16 and 17, respectively. For SP-NBR, the value of k_c or k_r seems to be nearly constant against the level of deformation: $k_c \doteq 0.028$, $k_r \doteq 0.033$. On the other hand, for SC-NBR, the value of k_c or k_r is a little larger than that for SP-NBR, and depends on the level of the deformation: $0.023 \leq k_c \leq 0.040$, $0.035 \leq k_r \leq 0.056$. In short-term failure, or at large deformation, k in Equation 22 is relatively large and some discussion would be needed about the influence of the values of k_c and k_r on the difference between the processes of creep and stress relaxation. According to Equation 22, the increment in k_c causes that in the value of m , and the increment in k_r causes the decrement in the value of m . Then, the relatively large values of k_c and k_r would explain qualitatively the difference between the value of m in the creep process and that in the stress relaxation process. The values of nk_c ($n < 4$) and

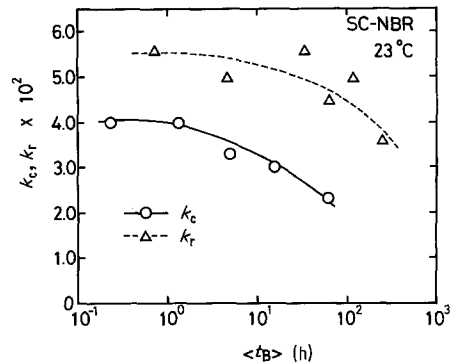


Figure 17 k_c and k_r plotted against $\langle t_B \rangle$ for SC-NBR. k_c , creep rate; k_r , stress relaxation rate; $\langle t_B \rangle$, mean lifetime.

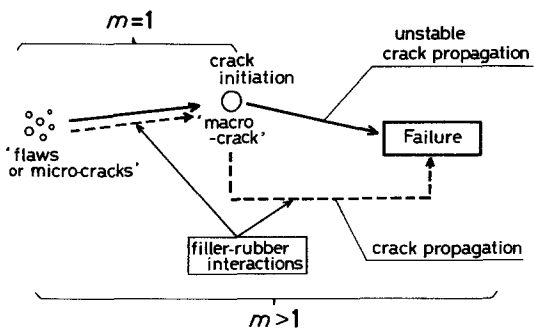


Figure 18 Failure behaviour under the constant stress state as a stochastic process: ———, for SP-NBR and for SC-NBR (short-term failure); - - - - -, for SC-NBR (long-term failure). m , Weibull modulus.

nk_T ($n < 10$), however, are small in comparison with those of m determined experimentally, and it is concluded that the contribution of viscoelasticity to the value of the Weibull modulus, $1 \leq m \leq 3$, is not so large as to modify the failure behaviour. Kawabata [10] similarly examined this effect of viscoelasticity on the creep failure of styrene-butadiene rubber (SBR), plasticized poly(vinyl chloride) (PVC), and NBR/PVC blends. He estimated by the calculation that this effect might not be considerable, even if not negligible. Thus, it is confirmed that the difference between the values of m , or the distributions of the lifetime, for rubber vulcanizates may be caused by the difference in their failure mechanisms.

From these results, the following model for static fatigue of rubber vulcanizates is presented, as shown in Fig. 18. As seen in this figure, the failure behaviour of pure vulcanizate (or carbon-reinforced vulcanizate in short-term failure) as the stochastic process is connected with the probabilistic initiation of an unstable crack, while that of carbon-reinforced vulcanizate in long-term failure as the stochastic process is connected with the probabilistic multi-crack initiation, accompanied by slow crack propagation; however, the period of crack propagation in the final stage of failure is small in comparison with the lifetime, t_B .

6. Conclusions

The failure mechanism of static fatigue of rubber vulcanizates was estimated by statistical analysis of the distribution of the lifetime. The stochastic theory, proposed by Kawabata *et al.* [8–10], was modified, and, on modification, a functional form of the Weibull distribution was derived for the

distribution of the lifetime of rubber vulcanizates: the theory could be applied to deal with the spatial distribution of flaws in the solid as well as the time dependence of the crack initiation leading to failure.

The failure mechanism of static fatigue of rubber vulcanizates is concluded as follows:

1. in pure vulcanizate, the random failure ($m = 1$) followed by the initiation and propagation of an unstable crack without delay occurs, in which a flaw or microcrack grows to some critical size. The failure behaviour appears to reflect the inherent characteristics of pure vulcanizate;

2. in carbon-reinforced vulcanizate, the failure behaviour depends on the stress state: in short-term failure, random failure occurs in similar way to that in pure vulcanizate. In long-term failure, wear-out failure occurs ($m \approx 3$), due to the energy loss or spatial effect near the tips of growing cracks in the presence of carbon black particles. In this case, the multi-crack initiation plays an important role;

3. finally, the authors present a model for the static fatigue of rubber vulcanizates, as shown in Fig. 18.

Although the statistical analysis introduced here may be an indirect method, the authors consider that this may be one of the most useful tools for examining various kinds of other effects, e.g. temperature, environmental effects, strain-induced crystallization, etc., on the failure behaviour. Furthermore, it is expected that this method will be applied to other studies and confirmed by further experiments, connecting the phenomenological study of the mechanical properties with the physical properties.

Acknowledgements

The authors wish to thank Professor S. Kawabata, Department of Polymer Chemistry, Faculty of Engineering, Kyoto University, for his advice and encouragement. They also thank Dr O. Kamigaito, Toyota Central Research and Development Laboratories, Inc, for his discussion.

References

1. M. HORI, *J. Phys. Soc. Japan* **14** (1959) 1444.
2. *Idem, ibid.* **17** (1962) 228.
3. B. D. COLEMAN, *J. Appl. Phys.* **28** (1957) 1058.
4. *Idem, ibid.* **28** (1957) 1065.
5. *Idem, ibid.* **29** (1958) 968.
6. I. NARISAWA and T. KONDO, *J. Polymer Sci. Polymer Phys. Ed.* **11** (1973) 1235.

7. H. H. KAUSCH, *J. Polymer Sci. Symp.* **32** (1971) 1.
8. S. KAWABATA and P. J. BLATZ, *Rubber Chem. Technol.* **39** (1966) 928.
9. S. KAWABATA, S. TATSUTA and H. KAWAI, in "Proceedings of the 5th International Congress on Rheology", edited by S. Onogi, Vol. 3 (University of Tokyo Press, Tokyo, 1970) p. 111.
10. S. KAWABATA, in "Durability of Macromolecular Materials", edited by R. K. Eby, ACS Symposium Series 95 (ACS, Washington, DC, 1979) p. 261.
11. G. P. WADSWORTH and G. P. BRYAN, "Introduction to Probability and Random Variables" (McGraw-Hill, New York, 1960).
12. W. FELLER, "An Introduction to Probability Theory and its Application", 2nd Ed., Vol. 1 (John Wiley, New York, 1957).
13. F. BUECHE, "Physical Properties of Polymers" (Interscience, New York, 1962).
14. G. M. BARTENEV and Y. S. ZUYEV, "Strength and Failure of Visco-elastic Materials" (Pergamon Press, Oxford, 1968).
15. E. H. ANDREWS, "Fracture in Polymers" (Oliver and Boyd, Edinburgh and London, 1968) p. 133.
16. E. J. GUMBEL, "Statistics of Extremes" (Columbia University Press, New York, 1958).
17. J. H. K. Kao, *J. Amer. Statist. Ass.* **51** (1956) 514.
18. T. YOKOBORI and Y. SAWAKI, *Int. J. Fracture* **9** (1973) 95.
19. Y. SAWAKI and T. YOKOBORI, *Rep. Res. Inst. Strength Fract. Mat. Tohoku Univ.* **9** (1973) 25.
20. A. R. PAYNE, *J. Polym. Sci. Symp.* **48** (1974) 169.

*Received 3 May
and accepted 24 October 1983*